The Ca^{2+}-induced Conformational Change of Gelsolin Is Located in the Carboxyl-terminal Half of the Molecule

T. Hellweg,* H. Hinssen,‡ and W. Eimer*§
*Department of Chemistry and ‡Biochemical Cell Biology Group, University of Bielefeld, 33675 Bielefeld, Germany

ABSTRACT We have purified the two functionally distinct domains of gelsolin, a Ca^{2+}-dependent actin binding protein, by proteolytic cleavage and characterized their size and shape in solution by dynamic light scattering. In the absence of calcium we obtained the same translational diffusion coefficient for both fragments which are of approximately equal molecular mass. The frictional ratio f_0/f_{exp} (1.33–1.39) is similar to the value as obtained for intact gelsolin (1.37) in aqueous solution (Patkowski, A., J. Seils, H. Hinssen, and T. Dorfmüller. 1990. *Biopolymers*. 30:427–435), indicating a similar molecular shape for the native protein as well as for the two subdomains. Upon addition of Ca^{2+} the translational diffusion coefficient of the carboxyl-terminal half decreased by almost 10%, while there was no change observed for the amino terminus. This result indicates that the ligand-induced conformational change as seen for intact gelsolin is probably located on the carboxyl-terminal domain of the protein. Since gelsolin has binding sites in both domains, and the isolated amino terminus binds and severs actin in a calcium-independent manner, our results suggests that the structural transition in the carboxyl-terminal part of intact gelsolin also affects the actin binding properties of the amino-terminal half.

INTRODUCTION

Gelsolin is a Ca^{2+}-dependent actin binding protein with both filament severing and barbed-end capping properties (1, 2). Gelsolin binds two Ca^{2+} with a K_d of 0.6–0.8 μM (3, 4). It also binds G-actin and forms ternary complexes with two actin molecules in the presence of Ca^{2+}. The binding of one of these actin molecules is EGTA-resistant, resulting in a stable binary complex at low calcium concentrations (<1 μM). Probably due to the complex formation with two actin molecules, gelsolin also promotes the nucleation of actin polymerization (5).

Spectroscopic measurements (6, 7) as well as immunological studies (8) have indicated that gelsolin undergoes conformational changes upon binding of Ca^{2+}. More detailed results from dynamic light scattering (DLS) measurements on intact gelsolin in solution have demonstrated that the shape of the molecule changes significantly: In the presence of EGTA, gelsolin is a clearly elongated molecule. The binding of Ca^{2+} ions results in a decrease of the rotational and translational diffusion coefficient, indicating a transition into a more open or unfolded conformation of the protein (9) which leads to a more spherical shape of the molecule.

Gelsolin as well as several related proteins like villin, fragmin, and severin show repeats in their amino acid sequence (10–14) suggesting that all proteins of this type have originated from a common 15-kDa ancestral precursor protein (10). Limited proteolysis of gelsolin by chymotrypsin or thermolysin generates two peptides with approximately equal molecular mass (15–17), each containing three of the repeating subdomains. Despite their related amino acid sequence, the two halves of the molecule have distinctly different functions: while the amino-terminal fragment retains the severing activity of the intact gelsolin but is no longer Ca^{2+}-sensitive, the carboxyl terminus binds actin in a Ca^{2+}-dependent manner but does not sever actin filaments (16, 17).

A more detailed analysis of fragments generated by deletion mutagenesis (4, 18–20) revealed that the amino-terminal domain contains two functional actin binding sites which act cooperatively for filament severing. The amino terminus can also bind Ca^{2+} and has a cryptic Ca^{2+}-binding site which is nonfunctional in intact gelsolin, (4) but confers Ca^{2+} sensitivity to some deletion mutants of the amino terminus (20). The precise location and nature of the Ca^{2+}-binding site in the carboxyl-terminal domain of gelsolin is still unknown. However, there is no indication for Ca^{2+}-binding sites of the EF-hand type.

In the present work, we have investigated the influence of Ca^{2+} on the conformation of the two gelsolin subdomains. We have purified the subdomains generated by chymotryptic cleavage, characterized them by photon correlation spectroscopy, and monitored their conformational changes upon addition of Ca^{2+}.

MATERIALS AND METHODS

Gelsolin preparation

Gelsolin was prepared from the smooth muscle of pig stomach by a procedure described by Hinssen et al. (21) and Pope et al. (22).

Limited proteolytic digestion of gelsolin and purification of fragments

Gelsolin (1 mg/ml in 5 mM Tris-HCl, pH 7.5, 1 mM $MgCl_2$, and 0.5 mM $CaCl_2$) was incubated with chymotrypsin at a weight ratio of 1:200 for approximately 60 s at 25°C. The reaction was terminated by the addition of 1 mM phenylmethylsulfonyl fluoride. (The precise time needed for optimal cleavage was calibrated for each batch of chymotrypsin.) This resulted in

Received for publication 19 November 1992 and in final form 24 March 1993.

Address reprint requests to Dr. Wolfgang Eimer, Fakultat Für Chemie, Universität Bielefeld, 33507 Bielefeld, Germany.

0006-3495/93/08/799/07 $2.00

a nearly complete cleavage of gelsolin into two peptides with an apparent molecular mass in sodium dodecyl sulfate-polyacrylamide gel electrophoresis (SDS-PAGE) of 40 and 43 kDa, respectively. Only minute amounts of peptides with lower molecular weight were generated under these conditions.

For separation and purification of the fragments the solution was subjected to anionic exchange chromatography on LiChrospher-TMAE (Merck). The smaller amino-terminal fragment eluted unbound, whereas the carboxyl terminus and uncleaved gelsolin were bound and eluted separately by a linear gradient of 100–400 mM KCl. Both fragments were concentrated and further purified by gel chromatography on Superdex G-200 (Pharmacia, Freiburg, Germany). To remove smaller amounts of aggregated material, the samples were centrifuged 3 h at 100,000 *g*.

Functional assays for gelsolin fragments

Severing activity of the amino-terminal domain was assayed by Ostwald viscometry as described for intact gelsolin (9). Calcium-sensitive actin binding of the carboxyl-terminal domain was verified by a sedimentation assay using skeletal muscle actin. Mixtures of F-actin and the 43-kDa carboxyl-terminal fragment (25:1 m/m) were centrifuged for 30 min at 100,000 *g* in an Airfuge (Beckman Instruments, Fullerton, CA). SDS samples revealed increasing amounts of actin in the supernatants in the presence of Ca^{2+}. Complex formation between the carboxyl-terminal domain and G-actin was also revealed by high-resolution gel chromatography on Superdex 200.

Dynamic light scattering measurements

The light scattering instrument used has been described in detail elsewhere (9). The argon ion laser was operated in single-mode at $\lambda = 488$ nm with an output power of 400 mW. Correlation functions were measured with a BI-2030 correlator from Brookhaven Instruments (Holtsville, NY) a temperature of 10°C. The angular dependence of the relaxation rate was monitored for scattering angles of 30° to 120°. Due to the low scattering intensity of the samples at low concentration, we used a "dust correction procedure" to account for the sporadically appearing high scattering intensities in the scattering volume. Correlation functions were measured for short periods of time and those with a difference between measured and calculated baseline $> 0.1\%$ were rejected. Addition of single spectra was continued up to 1×10^7 counts per channel. Data accumulation was controlled by an HP 9000/300 microcomputer.

Data analysis

In a standard photon correlation experiment one measures the intensity autocorrelation function $G^{(2)}(\tau)$ of scattered light. For the "Gaussian beam" approximation it is related to the normalized field autocorrelation function $g^{(1)}(\tau)$ by (23),

$$G^{(2)}(\tau) = B[1 + f|g^{(1)}(\tau)|^2] \tag{1}$$

where B is the baseline and f is a constant that depends on the scattering geometry. For a monodisperse sample of small molecules, undergoing Brownian diffusion, $g^{(1)}(\tau)$ is given by a single exponential,

$$g^{(1)}(\tau) = \exp(-\Gamma\tau) \tag{2}$$

with $\Gamma = Dq^2$, the mutual diffusion coefficient, and the wave vector $q = 4\pi n \sin(\theta/2)/\lambda_0$. Here, θ is the scattering angle, λ_0 the laser wavelength in vacuo, and n the refractive index of the sample.

For a polydisperse system $g^{(1)}(\tau)$ can be represented by a weighted sum of exponentials

$$g^{(1)}(\tau) = \int_0^\infty G(\Gamma)\exp(-\Gamma\tau)\, d\Gamma \tag{3}$$

where $G(\Gamma)$ describes the distribution of relaxation rates. Eq. 3 is also applicable to monodisperse samples, where a single exponential fit does not perfectly represent the measured correlation function. This might occur at low concentration of low molecular weight samples, like the protein studied here, where the incoherent solvent scattering and infrequently appearing stray light give a significant contribution to the total intensity of scattered light. Furthermore, it is possible to detect small amounts of high molecular weight impurities, e.g., aggregate structures.

The distribution of relaxation rates can be analyzed by the method of cumulants (24) or by an inverse Laplace transformation of Eq. 3 by the FORTRAN program CONTIN (25, 26) The weighted average diffusion coefficient can be calculated from the first cumulant (μ_1). The normalized second cumulant (μ_2/μ_1^2) is a measure for the width of distribution and polydispersity. The second cumulant is equal to the second moment from CONTIN. The CONTIN program is better capable to discriminate small contributions from "dust" than the method of cumulants, because it contains an additional linear coefficient in Eq. 3 that can account for stray light in the correlation function.

For a dilute solution of noninteracting molecules, the self diffusion coefficient is related to the hydrodynamic radius by the Stokes-Einstein equation,

$$D = \frac{kT}{6\pi\eta_0 r} \tag{4}$$

where k is the Boltzmann constant, η_0 the solvent viscosity, and r the radius of the spherical particle.

To a first approximation, the anisotropic shape of proteins can be modeled by an biaxial ellipsoid (a, b, b), with semiaxes a and b. The translational diffusion coefficient can be calculated by the Perrin equations (27, 28),

$$D = \frac{kT}{6\pi\eta_0 r} G(\rho) \tag{5}$$

$G(\rho)$ is a function of the axial ratio $\rho = b/a$. For an oblate ellipsoid ($a < b$; $\rho > 1$) the shape factor $G(\rho)$ is given by,

$$G(\rho) = (\rho^2 - 1)^{-1/2}\arctan[(\rho^2 - 1)^{1/2}] \tag{6}$$

and for a prolate ellipsoid ($a > b$; $\rho < 1$),

$$G(\rho) = (1 - \rho^2)^{-1/2}\ln\left[\frac{1 + (1 - \rho^2)^{1/2}}{\rho}\right] \tag{7}$$

To determine the semiaxes a and b, it is necessary to have information about both transport properties, the translational, and rotational diffusion coefficient. Nevertheless, knowledge of just the translational friction coefficient $f = kT/D$ provides the frictional ratio,

$$\frac{f}{f_0} = \frac{r}{r_0} = \frac{r}{(3M\nu/4\pi N_L)^{1/3}} \tag{8}$$

due to the asymmetry of the molecule. f_0 is the frictional coefficient of a compact sphere, where the radius is determined by the molecular weight, M, and the specific volume, ν, of the protein in solution. N_L is Avogadro' s number.

RESULTS

The described purification procedure for the gelsolin fragments yielded two polypeptides with apparent molecular masses in SDS-PAGE of 40 and 43 kDa, respectively (Fig. 1). These values are in good agreement with the actual molecular weight of 80.3 kDa for the cytoplasmic variant of gelsolin from pig as calculated from the amino acid sequence (10). As shown in Fig. 1, the purified peptides contained very little contamination of smaller peptides and no intact gelsolin. The amino-terminal domain appeared slightly heterogenous on SDS-PAGE and seemed to consist of two bands with a very small difference in apparent molecular weight

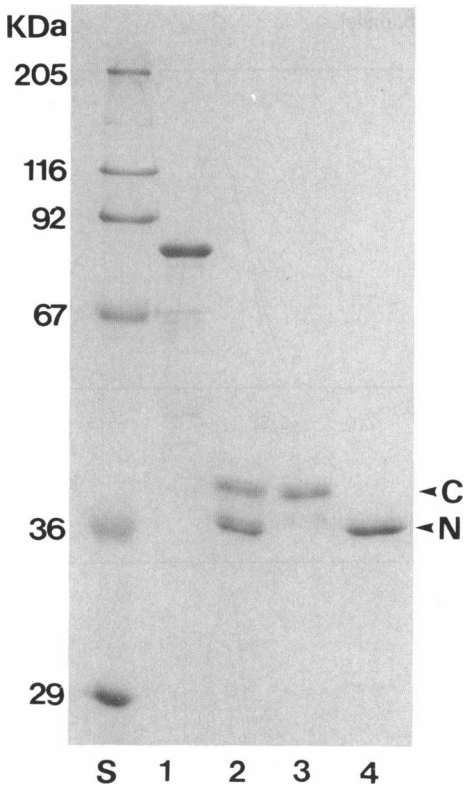

FIGURE 1 SDS-PAGE of pig stomach gelsolin and its proteolytic fragments generated by chymotrypsin. (*1*) Purified gelsolin; (*2*) gelsolin after incubation with chymotrypsin for 60 min; (*3*) purified amino-terminal domain; (*4*) purified carboxyl-terminal domain. Numbers indicate the positions of molecular weight markers.

(Fig. 1, *lane 3*). The functional identity of the fragments was checked by monitoring the Ca^{2+}-independent actin filament severing property of the amino-terminal domain and the Ca^{2+}-sensitive actin binding of the carboxyl terminus. Furthermore, by dynamic light scattering measurements it was verified that after gel filtration all traces of high molecular weight material, possibly aggregates of denatured protein, were absent.

After characterization of the purity and biological activity, we studied the hydrodynamic properties of both the amino-terminal and carboxyl-terminal gelsolin domains by photon correlation spectroscopy. For the carboxyl terminus, under calcium free conditions (0.1 mM EGTA), Fig. 2 indicates that up to 1 mg/ml the mutual diffusion coefficient was independent on concentration. According to the following,

$$D_0 = D_w^{20}(1 + k \cdot c) \qquad (9)$$

the self-diffusion coefficient D_0 is obtained by extrapolation to zero concentration. For the carboxyl-terminal fragment the intercept gave $D_w^{20} = (7.0 \pm 0.15) \times 10^{-7}$ cm^2/s. From the DLS experiments on the amino-terminal subdomain we obtained almost the same translational diffusion coefficient. Fig. 2 reveals that the experimental data at various concentrations seemed to be always smaller than for the carboxyl terminus, indicating a lower self diffusion coefficient of

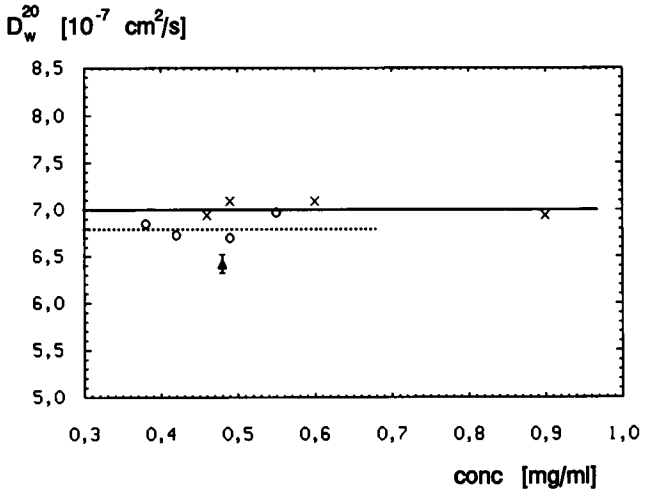

FIGURE 2 Concentration dependence of the translational diffusion coefficient for the two gelsolin subfragments as obtained from limited proteolysis by thermolysin. (○) Amino-terminal domain, (×) carboxyl-terminal domain; without calcium. For the carboxyl terminus the results were obtained from two different protein preparations. (▲) Carboxyl-terminal domain with calcium. The experimental data are corrected for T = 20°C.

$D_w^{20} = (6.8 \pm 0.15) \times 10^{-7}$ cm^2/s. However, considering the experimental error, the difference is not significantly large enough for a distinctive differentiation, but it could reflect the lower apparent molecular weight of the amino-terminal fragment according to SDS-PAGE (see Fig. 1).

For a given concentration, we have performed photon correlation experiment at different scattering angles. According to $\Gamma = Dq^2$, (see Eq. 2), the relaxation rate Γ is expected to depend on the square of the scattering angle θ. For both proteolytic fragments, Fig. 3 shows Γ as a function of q^2 for a scattering angle of $30° \leq \theta \leq 120°$. The straight lines indicate that we followed the translational motion of the

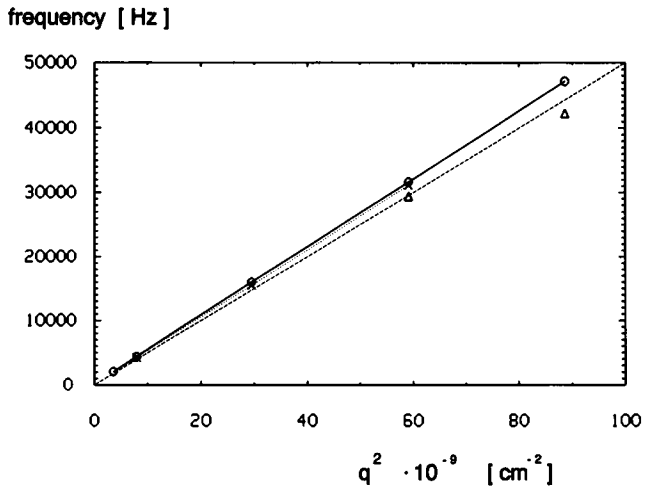

FIGURE 3 Angular dependence of the relaxation rate Γ for the two subdomains of gelsolin. (×) Amino terminus; (○) carboxyl terminus; (▲) carboxyl terminus with calcium.

polypeptides in solution and the mutual diffusion coefficient was obtained from the slope. Again, the slope for the amino terminus appears to be smaller than for the carboxyl terminus. But considering the experimental error in the mutual diffusion coefficients, in the following discussion, we will assume the same value for both subdomains under calcium free conditions.

To verify the influence of Ca^{2+} on the diffusion coefficient, and hence on the hydrodynamic dimensions, we added $CaCl_2$ to a final concentration of 0.2 mM to a solution of the amino-terminal fragment (0.38 mg/ml). By inverse Laplace transformation we obtained a diffusion coefficient of $D_w^{20} = (6.95 \pm 0.15) \times 10^{-7}$ cm^2/s, which is identical to the result in EGTA solution. Therefore, we may conclude that the binding of Ca^{2+} does not significantly change the size and shape of the amino-terminal subdomain of gelsolin.

We have repeated the same experiments on the carboxyl half of the protein. For these measurements we prepared an additional sample by digestion of gelsolin with chymotrypsin to verify the reproducibility of our hydrodynamic studies. As Fig. 2 reveals, under calcium free conditions in the presence of EGTA the experimental data for two different preparations of the carboxyl terminus are identical within experimental error. However, upon addition of Ca^{2+} the translational diffusion coefficient changed from $D_w^{20} = (7.0 \pm 0.15) \times 10^{-7}$ cm^2/s to $D_w^{20} = (6.4 \pm 0.15) \times 10^{-7}$ cm^2/s which indicates a change in the hydrodynamic dimensions of the carboxyl-terminal domain. Due to the small decrease of the diffusion coefficient, we carefully checked the reproducibility of our results on the same sample at different scattering angles (see Fig. 3). Additional measurements on a different preparation of the carboxyl terminus confirmed the change in the diffusion coefficient.

Fig. 4 shows a typical distribution of diffusion coefficients as obtained from the intensity autocorrelation function by CONTIN analysis. The line width is a measure for a possible heterogeneity of the sample, due to isoforms of the protein, aggregate formation, or denaturation. The normalized variance for the carboxyl-terminal domain was calculated to $\mu_2/\mu_1^2 = 0.07$, where $\mu_1 = \Gamma = G(\Gamma)\,\Gamma\,d\Gamma$ and $\mu_2 = G(\Gamma)\,(\Gamma - \Gamma)^2\,d\Gamma$. Considering the rather low intensity of scattered light, due to the relatively low molecular weight of the molecules, this indicates a monodisperse sample, and we can neglect the presence of different conformational or aggregate structures. Addition of 0.2 mM Ca^{2+} to the fragment in solution did not result in a significant broadening of the distribution function and hence, we can conclude that the binding of calcium does not increase the heterogeneity of the sample. A comparison of Fig. 4, *a* and *b*, reveals an increase in the normalized variance to about $\mu_2/\mu_1^2 = 0.11$ for the amino-terminal fragment. The slightly broader distribution of diffusion coefficients is probably related to the small heterogeneity in the molecular weight of the amino terminus.

As seen in Fig. 4, the inverse Laplace transformation of the DLS spectra for the carboxyl-terminal subdomain with added Ca^{2+} gave a second relaxation mode with a much slower relaxation rate and a small amplitude (less than 2%). This

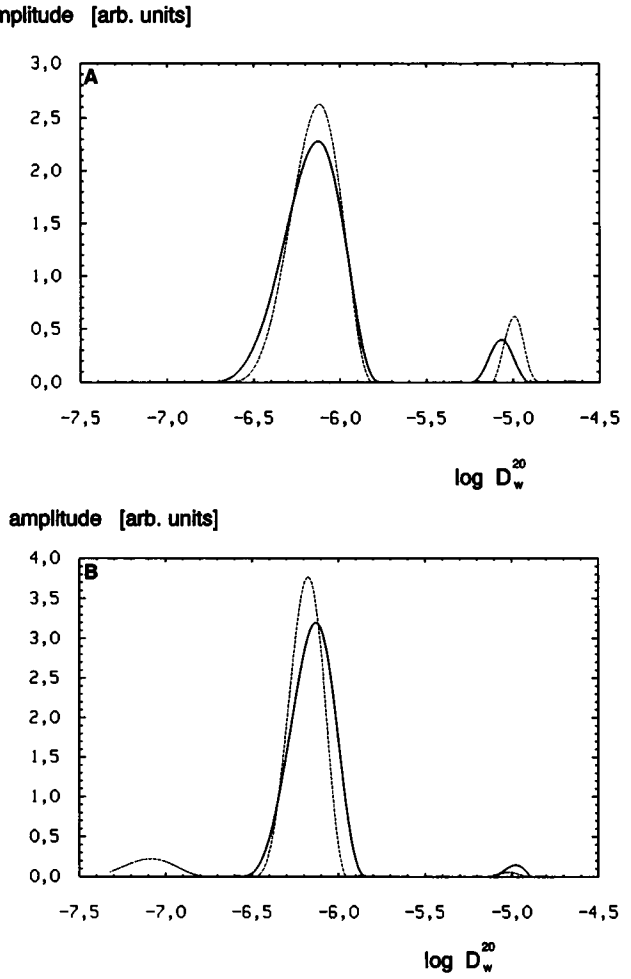

FIGURE 4 Distribution of translational diffusion coefficients from the intensity autocorrelation function as obtained from CONTIN analysis. (*a*) Amino-terminal subdomain of gelsolin; (- - -) with and (—) without calcium. (*b*) Carboxyl-terminal subdomain of gelsolin; (- - -) with and (—) without calcium.

probably indicates some aggregate formation on addition of $CaCl_2$, but does not interfere with the interpretation of the dynamics of the carboxyl-terminal subdomain in respect to a conformational transition. The small peak at the high end of the distribution functions for all fragments is a numerical artefact, often observed in the CONTIN analysis.

DISCUSSION

Dynamic light scattering studies on gelsolin (9) have shown that calcium binding results in a large conformational transition of the molecule to a more spherical but also more extended shape in solution. The axial ratio of the hydrodynamically equivalent ellipsoid of revolution changes from $\rho = 0.25$ to $\rho = 0.40$, whereas the apparent volume increases from 153 to 314 Å^3. This massive conformational change can be interpreted as a partial rearrangement in the polypeptide chain, leading to a more unfolded tertiary structure of the intact gelsolin molecule. Due to this rearrangement, the actin binding sites on the amino terminus could be exposed which

were masked in the absence of Ca^{2+}. By limited proteolysis of gelsolin we separated the two halves of the protein. Using dynamic light scattering on these fragments we wanted to test whether the calcium-induced conformational change is restricted to one of the subdomains or if both parts of the molecule are involved in a cooperative manner.

A comparison of the DLS results for intact gelsolin (9) and its subdomains is given in Table 1. As expected, the translational diffusion coefficient for gelsolin is significantly smaller than for the two fragments, illustrating the difference in molecular weight. For the amino terminus we did not observe any change in the translational diffusion coefficient upon addition of calcium. This result indicates that the molecular dimensions of the structural subdomain do not change significantly. For the carboxyl terminus, however, the presence of Ca^{2+} ions resulted in a decrease of the translational diffusion coefficient by about 10% which is similar to the effect observed for intact gelsolin.

To characterize the structural change induced by binding of the divalent cation, we will compare the experimental data with theoretical calculations on spherical models of the same molecular weight as gelsolin and its subdomains. According to the following,

$$r_{sph} = \frac{1}{2}\left(\frac{6M\nu}{\pi N_A}\right)^{1/3} \tag{10}$$

we have calculated the hydrodynamic radii for compact spheres, where M is the molecular weight and N_L the Avogadro number. For the partial specific volume of the protein we used $\nu = 0.73$ ml/g. From r_{sph} we can determine the theoretical diffusion coefficient, D_w^{20}, as expected for a spherical molecule, according to the Stokes-Einstein relation (Eq. 4), for all species studied. In Table 1 we have also included the theoretical translational diffusion coefficients for the hydrated protein molecules. The thickness of the hydration layer was assumed to 0.3 nm as found in most hydrodynamic studies (29, 30).

A comparison of the theoretical values with experimental data gives a clue to the anisotropic structure of the molecules. When the calcium level is below 10^{-6} mol/liter, the molecular dimensions of hydrated gelsolin were determined to $a = (8.3 \pm 0.4)$ nm and $b = (2.1 \pm 0.2)$ nm, assuming an ellipsoidal shape for the molecule. Addition of Ca^{2+} results in a conformational transition to a more spherical structure with $a = (7.8 \pm 0.5)$ nm and $b = (3.1 \pm 0.3)$ nm. The transition is cooperative (Hellweg, Hinssen, and Eimer, unpublished data) and is accompanied by a significant increase in the hydrodynamic volume from 153 to 314 Å^3. Usually, a decrease in the form anisotropy of a molecule gives a smaller shape factor in the Perrin equations, and therefore results in a larger diffusion coefficient. In our case, upon addition of calcium ions gelsolin adopts a more spherical shape but the increase in the hydrodynamic volume leads to a decrease in the translational diffusion coefficient. Therefore, the larger ratio of the frictional coefficients f_0/f_{exp} (see Table 1) for gelsolin in the presents of Ca^{2+} does not indicate a more anisotropic structure of the molecule in solution. It is simply a measure of structural change of the protein induced by ligand binding. If we compare the ratio of the frictional coefficients for gelsolin and both subdomains without calcium they are very similar. Assuming that the specific volume for all three species does not vary significantly, we can conclude that the axial ratios of both the carboxyl and the amino terminus are similar to that of intact gelsolin, indicating an elongated shape for all three molecules.

While calcium has no detectable effect on the amino-terminal subdomain, the translational diffusion coefficient of the carboxyl terminus decreases upon addition of Ca^{2+}. That means, the conformational change of intact gelsolin on ligand binding is located mainly on the carboxyl terminus. The increase in f_0/f_{exp} from 1.33 to 1.46 is similar to the effect observed for intact gelsolin (for comparison see Table 1). As already discussed for gelsolin, an increase in the ratio of the frictional coefficients does not necessarily indicate a change to a more anisotropic structure of the molecule. However, it may be inferred from our results with intact gelsolin that also the carboxyl terminus undergoes a rearrangement in the folding of the polypeptide chain leading to a more extended structure which finally results in a more spherical shape of this fragment. Because of the low scattering intensity of the proteolytic fragments, we were not able to do depolarized dynamic light scattering experiments as for intact gelsolin. With

TABLE 1 Comparison of hydrodynamic properties for gelsolin and its carboxyl-terminal and amino-terminal subdomains

	Gelsolin[a]		Amino terminus		Carboxyl terminus		
	$+Ca^{2+}$	$-Ca^{2+}$	$+Ca^{2+}$	$-Ca^{2+}$	$+Ca^{2+}$	$-Ca^{2+}$	Units
M_r[b]	84,000		40,000		43,000		Da
r_s[c]	2.90		2.22		2.30		nm
D_w^{20}(theor)[d]	7.40 (6.71)		9.50 (8.39)		9.34 (8.26)		$\times 10^{-7}$ cm^2/s
D_w^{20}(exp)	4.70	5.50	6.95	6.80	6.40	7.00	$\times 10^{-7}$ cm^2/s
r(exp)	4.55	3.90	3.15	3.1	3.4	3.1	nm
f_0/f_{exp}	1.57	1.37	1.38		1.46	1.33	

[a] From Patkowski et al., 1990.

[b] Apparent molecular weight in SDS-gel electrophoresis.

[c] Calculated according to Eq. 10.

[d] Calculated according to Eq. 4; values in parentheses correspond to the hydrated structures, the thickness of the hydration layer was assumed to 0.3 nm.

the information on the rotational diffusion coefficients we could have calculated the axial ratio for the amino-terminal and carboxyl-terminal domains, and hence characterized the potential change in shape of the domains under the influence of calcium.

The binding of calcium to gelsolin or the carboxyl-terminal fragment is probably also related to a rearrangement of the solvent structure in the immediate vicinity of the protein molecule. This effect could partly account for the increase of the hydrodynamic volume as observed for intact gelsolin. However, we do not observe a comparable increase in the hydrodynamic volume for the amino terminus. Therefore, we conclude that the major part of the conformational transition is related to a change in the tertiary structure of the protein itself.

A significant conformational change upon binding of Ca^{2+} has been reported for villin (31). It has been shown that this change resides in the 8-kDa villin-specific carboxyl-terminal "headpiece" region which has an additional actin binding site responsible for the actin filament bundling property of villin (32). However, in contrast to our findings for gelsolin, Ca^{2+} binding lead to a considerable increase in asymmetry of the villin molecule with the apparent length increasing from 8.9 to 12.3 nm. Therefore, it is not clear whether the changes observed for gelsolin and villin are related processes.

It is evident from previous biochemical experiments (15–17) that the carboxyl-terminal half of gelsolin confers Ca^{2+} sensitivity of actin binding to the whole molecule. From our data it can be concluded that it is the observed conformational transition upon binding of Ca^{2+} that prevents the binding of actin to all three operative binding sites of gelsolin. Two of these actin binding sites are located in the amino-terminal half (10, 15, 33), one within the first 150 amino acid residues (18, 19). A possible explanation for this phenomenon is that the binding sites in the amino-terminal half of gelsolin are masked by parts of the carboxyl-terminal polypeptide chain in the absence of Ca^{2+} and that binding of Ca^{2+} induces a rearrangement in the conformation of the whole molecule that unmasks the binding sites for actin. The fact that only the carboxyl-terminal domain of gelsolin undergoes a Ca^{2+}-induced conformational change excludes possible models which assume that, due to a flexible hinge region in the molecule, the two conformationally invariant domains change their relative position, and thereby induce the massive conformational transition in the protein (4, 34).

We gratefully acknowledge financial support from the Deutsche Forschungsgemeinschaft (SFB 223).

REFERENCES

1. Vandekerckhove, J., and K. Vancompernolle. 1992. Structural relationships of actin binding proteins. *Curr. Opin. Cell Biol.* 4:36–42.
2. Hartwig, J. H., and D. J. Kwiatkowski. 1991. Actin binding proteins. *Curr. Opin. Cell Biol.* 3:87–97.
3. Yin, H., and T. P. Stossel. 1980. Purification and structural properties of gelsolin, a Ca- activated regulatory protein of macrophages. *J. Biol. Chem.* 255:9490–9443.
4. Way, M., J. Gooch, B. Pope, and A. G. Weeds. 1989. Expression of human plasma gelsolin in Escherichia coli and dissection of actin binding sites by segmental deletion mutagenesis. *J. Cell Biol.* 109:593–605.
5. Janmey, P. A., C. Chaponnier, S. E. Lind, K. S. Zaner, T. P. Stossel, and H. L. Yin. 1985. Interactions of gelsolin and gelsolin-actin complexes with actin. Effects of calcium on actin nucleation, filament severing, and end blocking. *Biochemistry.* 24:3714–3723.
6. Kilhoffer, M. C., and D. Gerard. 1985. Fluorescence study of brevin, the Mr 92 000 actin-capping and -fragmenting protein isolated from serum. Effect of Ca^{2+} on protein conformation. *Biochemistry.* 24:5653–5660.
7. Rouayrenc, J. F., A. Fattoum, C. Mejean, and R. Kassab. 1986. Characterization of the Ca^{2+}-induced conformational changes in gelsolin and identification of interaction regions between actin and gelsolin. *Biochemistry.* 25:3859–3867.
8. Hwo, S., and J. Bryan. 1986. Immuno-identification of Ca^{2+}-induced conformational changes in human gelsolin and brevin. *J. Cell Biol.* 102:227–236.
9. Patkowski, A., J. Seils, H. Hinssen, and T. Dorfmüller. 1990. Size, shape, and Ca^{2+}- induced conformational change of the gelsolin molecule: a dynamic light scattering study. *Biopolymers.* 30:427–435.
10. Way, M., and A. Weeds. 1988. Nucleotide sequence of pig plasma gelsolin. Comparison of protein sequence with human gelsolin and other actin-severing proteins shows strong homologies and evidence for large internal repeats. *J. Mol. Biol.* 203:1127–1133.
11. Bazari, W. L., P. Matsudaira, M. Wallek, T. Smeal, R. Jakes, and Y. Ahmed. 1988. Villin sequence and peptide map identify six homologous domains. *Proc. Natl. Acad. Sci. USA.* 85:4986–4990.
12. Arpin, M., J. Prigault, A. Finidori, J. M. Garcia, J. Jeltsch, J. Vanderkerckhove, and D. Louvard. 1988. Sequence of human villin: a large duplicated domain homologous with other actin-severing proteins and a unique small carboxy-terminal domain related to villin specifity. *J. Cell Biol.* 107:1759–1766.
13. Andre, E., F. Lottspeich, M. Schleicher, and A. Noegel. 1988. Severin, gelsolin, and villin share a homologous sequence in regions presumed to contain F-actin severing domains. *J. Biol. Chem.* 263:722–727.
14. Yin, H. L., P. A. Janmey, and M. Schleicher. 1990. Severin is a gelsolin prototype. *FEBS Lett.* 264:78–80.
15. Kwiatkowski, D. J., P. A. Janmey, J. E. Mole, and H. L. Yin. 1985. Isolation and properties of two actin-binding domains in gelsolin. *J. Biol. Chem.* 260:15232–15238.
16. Chaponnier, C., P. A. Janmey, and H. L. Yin. 1986. The actin filament-severing domain of plasma gelsolin. *J. Cell Biol.* 103:1473–1481.
17. Bryan, J., and S. Hwo. 1986. Definition of an amino-terminal actin-binding domain and a carboxyl-terminal Ca^{2+} regulatory domain in human brevin. *J. Cell Biol.* 102:1439–1446.
18. Way, M., B. Pope, J. Gooch, M. Hawkins, and A. G. Weeds. 1990. Identification of a region in segment 1 of gelsolin critical for actin binding. *EMBO J.* 9:4103–4109.
19. Way, M., B. Pope, and A. G. Weeds. 1992. Are the conserved sequences in segment 1 of gelsolin important for binding actin? *J. Cell Biol.* 116: 1135–1143.
20. Kwiatkowski, D. J., P. A. Janmey, and H. L. Yin. 1989. Identification of critical functional and regulatory domains in gelsolin. *J. Cell Biol.* 108:1717–1726.
21. Hinssen, H., J. V. Small, and A. Sobieszek. 1984. A Ca^{2+}-dependent actin modulator from vertebrate smooth muscle. *FEBS Lett.* 166:90–95.
22. Pope, B., J. Gooch, H. Hinssen, and A. G. Weeds. 1989. Loss of calcium sensitivity of plasma gelsolin is associated with the presence of calcium ions during preparation. *FEBS Lett.* 259:185–188.
23. Berne, B. J., and R. Pecora. 1976. Dynamic light scattering. John Wiley & Sons, Inc., New York.
24. Koppel, D. E. 1972. Analysis of macromolecular polydispersity in intensity correlation spectroscopy: the methods of cumulants. *J. Chem. Phys.*. 57:4814–4820.
25. Provencher, S. W. 1982. A constrained regularization method for inverting data represented by linear algebraic or integral equations. *Comput. Phys. Commun.*, 27:213–227.
26. Provencher, S. W. 1982. CONTIN: a general purpose constrained regularization program for inverting linear algebraic and integral equations. *Comput. Phys. Commun.*, 27:229–242.

27. Perrin, F. 1934. Mouvement Brownian d 'un ellipsoide. I. Dispersion dielectrique pour des molecules ellipsoidales. *J. Phys. Radium*, 5:497–511.

28. Perrin, F. 1936. Mouvement Brownian d'un ellipsoide. II. Rotation libre et depolarisation des fluorescences. Translation et diffusion de molecules ellipsoidales. *J. Phys. Radium*, 7:1–11.

29. Dubin, S. B., N. A. Clark, and G. B. Benedek. 1971. Measurement of the rotational diffusion coefficient of lysozyme by depolarized light scattering: configuration of lysozyme in solution. *J. Chem. Phys.* 54: 5158–5164.

30. Eimer, W., M. Niermann, M. Eppe, and B. M. Jockusch. 1992. Molecular shape of vinculin in aqueous solution. *J. Mol. Biol.* 229:146–152.

31. Hesterberg, L. K., and K. Weber.1983. Ligand-induced conformational changes in villin, a calcium-controlled actin modulating protein. *J. Biol. Chem.* 258:359–364.

32. Janmey, P. A., and Matsudaira, P. T. 1988. Functional comparison of villin and gelsolin. Effects of Ca2+, KCl and polyphosphoinositides. *J. Biol. Chem.* 263:16738–16743.

33. Bryan, J. 1988. Gelsolin has three actin-binding sites. *J. Cell Biol.* 106:1553–1562.

34. Vandekerckhove, J. 1990. Actin binding proteins. *Curr. Opin. Cell Biol.* 2:40–50.